China Ocean Eng., Vol. 27, No. 5, pp. 593 – 604

DOI 10.1007/s13344-013-0050-8, ISSN 0890-5487

Solitary Wave Propagation Influenced by Submerged Breakwater*

WANG Jin (王　锦)[a, 1], ZUO Qi-hua (左其华)[a]

WANG Deng-ting (王登婷)[a] and Shirin Shukrieva[b]

[a] *Nanjing Hydraulic Research Institute*, *Nanjing 210029*, *China*

[b] *Bulgarian Academy of Sciences, Bulgarian Ship Hydrodynamics Centre, Varna, Bulgaria*

(Received 6 June 2012; received revised form 18 October 2012; accepted 28 February 2013)

ABSTRACT

The form of Boussinesq equation derived by Nwogu (1993) using velocity at an arbitrary distance and surface elevation as variables is used to simulate wave surface elevation changes. In the numerical experiment, water depth was divided into five layers with six layer interfaces to simulate velocity at each layer interface. Besides, a physical experiment was carried out to validate numerical model and study solitary wave propagation. "Water column collapsing" method (WCCM) was used to generate solitary wave. A series of wave gauges around an impervious breakwater were set-up in the flume to measure the solitary wave shoaling, run-up, and breaking processes. The results show that the measured data and simulated data are in good agreement. Moreover, simulated and measured surface elevations were analyzed by the wavelet transform method. It shows that different wave frequencies stratified in the wavelet amplitude spectrum. Finally, horizontal and vertical velocities of each layer interface were analyzed in the process of solitary wave propagation through submerged breakwater.

Key words: *solitary wave*; *submerged breakwater*; *wavelet spectrum*; *propagation characteristics*; *Boussinesq equation*

1. Introduction

Solitary wave is a kind of fluctuation phenomenon which often happens in shallow water. In estuarine and coastal engineering, solitary wave can be used to describe certain characteristics of the long wavelength surface waves and waves caused by tsunamis and storm. The extreme waves which propagate to shallow sea will deform due to the variation of water depth, the bottom friction, and obstacles. Usually, the deformed waves which have high flow velocity and wave amplitude in nearshore area can release enormous energy during breaking and run-up processes. So it may bring about casualty and property damage. In order to reduce extreme wave's damage, it is very necessary to study on solitary wave propagation influenced by submerged breakwater.

Until now, many researches on solitary wave propagation have been published. Synolakis (1987) simulated solitary wave run-up process and verified the theoretical results. Zelt (1991) simulated the highest run-up and surface elevation change of solitary waves in laboratory. Hara *et al*. (1992) studied wave breaking characteristics of a solitary wave caused by a submerged obstacle by performing intensive numerical simulations using boundary integral method. Grilli *et al*. (1994) simulated the free

* The research was supported by the foundation "China Seawall Safety Risk Zoning and Storm Surge Envelope Diagram" (Grant No. 200101061) by the Ministry of Water Resources, China.

1 Corresponding author. E-mail: wangjin@nhri.cn

surface change of different initial solitary waves during shoaling. Li and Raichlen (2001, 2002) carried out an experiment to study solitary wave shoaling process. Penchev and Shukrieva (2007) established a finite water depth limit generating system of solitary waves in laboratory wave flume. In addition, a two-dimensional CFD numerical model was established. SPH method (Kim and Ko, 2008) was also used to simulate solitary wave propagation on a vertical wall and a sloping wall. Hsiao *et al*. (2010) investigated tsunami-like solitary waves impinging and overtopping an impermeable trapezoidal seawall on a 1:20 sloping beach by laboratory experiment and numerical model (two-dimensional volume of fluid type model). Although lots of researches have been carried out, those studies on solitary wave were mainly restricted to the surface elevation.

As known to all, wave gauges can provide time-dependent record of surface elevation. However, in many cases the most significant information is hidden in the frequency spectrum, which provides the energy associated with each frequency. In coastal and ocean engineering, the Fourier transform (FT) is usually used to obtain the frequency spectrum. The FT provides information on the number of frequency components, rather than when (in time) the particular frequency components occur. Such information is sufficient for the stationary signals as their frequency contents do not change over time and all the frequency components exist all the time (Massel, 2001). Solitary waves generated by WCCM are transient phenomena. There is energy transfer and dissipation through nonlinear interaction between different wave components during the propagation. We need to obtain information on the change of frequencies in the time domain. The wavelet transform (WT) can provide the time localization of the spectral components. Panizzo *et al*. (2002) illustrated in detail its capability to analyze aerial landslide-generated waves. Dong *et al*. (2010) also used WT method to analyze landslide-generated impact waves including components with solitary and dispersive wave characteristics. In consideration of the advantages of the WT for analyzing such non-stationary processes, it was chosen as the analysis method in our study. And horizontal and vertical velocities of every level changes in the process of solitary wave propagating through submerged breakwater were analyzed.

This paper is organized as follows: Section 2 presents governing equations of numerical model; Section 3 describes the experiment and then validates the numerical model; Section 4 investigates solitary wave propagation characteristics, such as wavelet amplitude spectra and layer interface velocity. Finally, conclusions are drawn in Section 5.

2. Numerical Model Set-up

Based on continuity equation and Euler equation, the form of Boussinesq equation which was proposed by Nwogu (1993) can be written as:

$$\eta_t+\nabla\cdot\left[\left(h+\varepsilon\eta\right)u_\alpha\right]+\mu^2\nabla\cdot\left\{\left(\frac{z_\alpha^2}{2}-\frac{h^2}{6}\right)h\nabla\left(\nabla\cdot u_\alpha\right)+\left(z_\alpha+\frac{h}{2}\right)h\nabla\left[\nabla\cdot\left(hu_\alpha\right)\right]\right\}=0\,; \tag{1}$$

$$u_t+\nabla\eta+\varepsilon\left(u_\alpha\cdot\nabla\right)u_\alpha+\mu^2\left\{\frac{z_\alpha^2}{2}\nabla\left(\nabla\cdot u_{\alpha t}\right)-z_\alpha\nabla\left[\nabla\cdot\left(hu_{\alpha t}\right)\right]\right\}=0\,, \tag{2}$$

where η is the wave surface elevation; $\nabla=(\partial x,\partial y)$ is the horizontal gradient operator; h is the

water depth; g is the gravitational acceleration; $\varepsilon = A/h$ and $\mu = h/L$ represent the nonlinearity and frequency dispersion, respectively, A, h, and L representing the typical amplitude, typical depth, and typical wavelength, respectively; u_α is the horizontal velocity at an arbitrary elevation z_α ($z_\alpha = -0.531h$).

In addition to the equations shown above, we need to put extended terms: friction, breaking, subgrid mixing, and absorbing boundary (Kennedy *et al*., 2000; Chen *et al*., 2000).

The depth in the vertical direction was divided into five layers with six lay interfaces as $z = -(\eta+h)$, $-0.8(\eta+h)$, $-0.6(\eta+h)$, $-0.4(\eta+h)$, $-0.2(\eta+h)$, and 0 and velocity at each layer interface was calculated.

3. Numerical Model Validation

The experiment was carried out in the water flume of River and Harbor Engineering Department of Nanjing Hydraulic Research Institute, China. The water flume is 175 m long, 1.2 m wide and 1.8 m deep and three kinds of water tanks for storing water column are placed at one side of water flume to generate solitary wave (WCCM)(Wang *et al*., 2011). The tank dimensions are 1.20 m×0.15 m×0.9 m, 1.2 m×0.35 m×0.9 m, and 1.2 m×0.55 m×0.9 m, respectively. An impervious breakwater was placed 20 m from the tank. The crest width of breakwater was 2 m and the slopes were 1:5. The crest elevation was 0.3 m, with the water depth being 0.4 m. Wave height data were collected by a series of wave gauges and post processed by computer automatically.

The waveform changes of solitary wave were simulated by the model. In order to prevent the wave reflection influence on the simulation, sponge layers boundary conditions were set up at both sides of the computation domain. In order to satisfy the convergence of the equation, a wave length is usually divided into 30–40 space steps. Time step Δt needs to be $\Delta t \le 0.5\min(\sqrt{\Delta x^2 + \Delta y^2}/\sqrt{gh})$. Therefore, the computational grid was 0.02 m, and the time step was 0.002 s in the simulation, with the entire simulation time being 28 s. Fig. 1 shows the layout of wave height gauges. The distances from gauges 1–11 to the tank (wave maker) were 10 m, 15 m, 17 m, 18.5 m, 19.25 m, 20 m, 20.5 m, 21 m, 21.5 m, 21.8 m, and 29 m, respectively.

Because a series of sub-waves were produced after the largest wave in the process of solitary wave generation (Wang *et al*., 2011), the first largest wave was analyzed only. Comparisons of calculated results with measured data are plotted in Fig. 2.

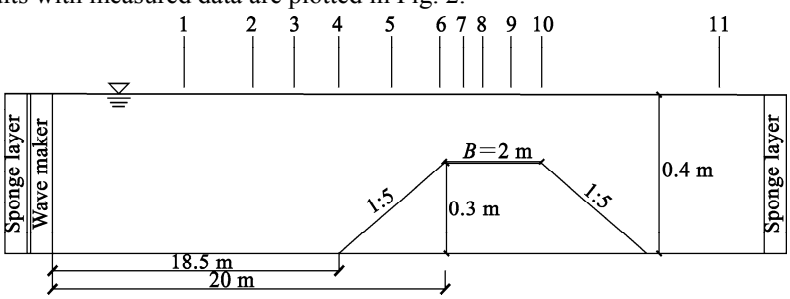

Fig. 1. Layout of wave height gauges.

Fig. 2 shows that the waveform of solitary wave remains unchanged at the beginning during propagation, the wave surface elevations are all above the still water level, and the wave height attenuations are not obvious. With the solitary wave propagating over the submerged breakwater, the water depth decreases and the wave height increases gradually, and then the waveform distorts forward until breaking. There are two causes: on the one hand, the wave steepness increases rapidly when the wave propagates through the submerged breakwater; on the other hand, the celerity of the crest of solitary wave is larger than that of the wave trough of solitary wave, because the celerity of solitary wave depends on water depth. So the crest of solitary wave moves to catch the wave trough gradually. The waveform distorts and breaks when the wave steepness reaches its limit.

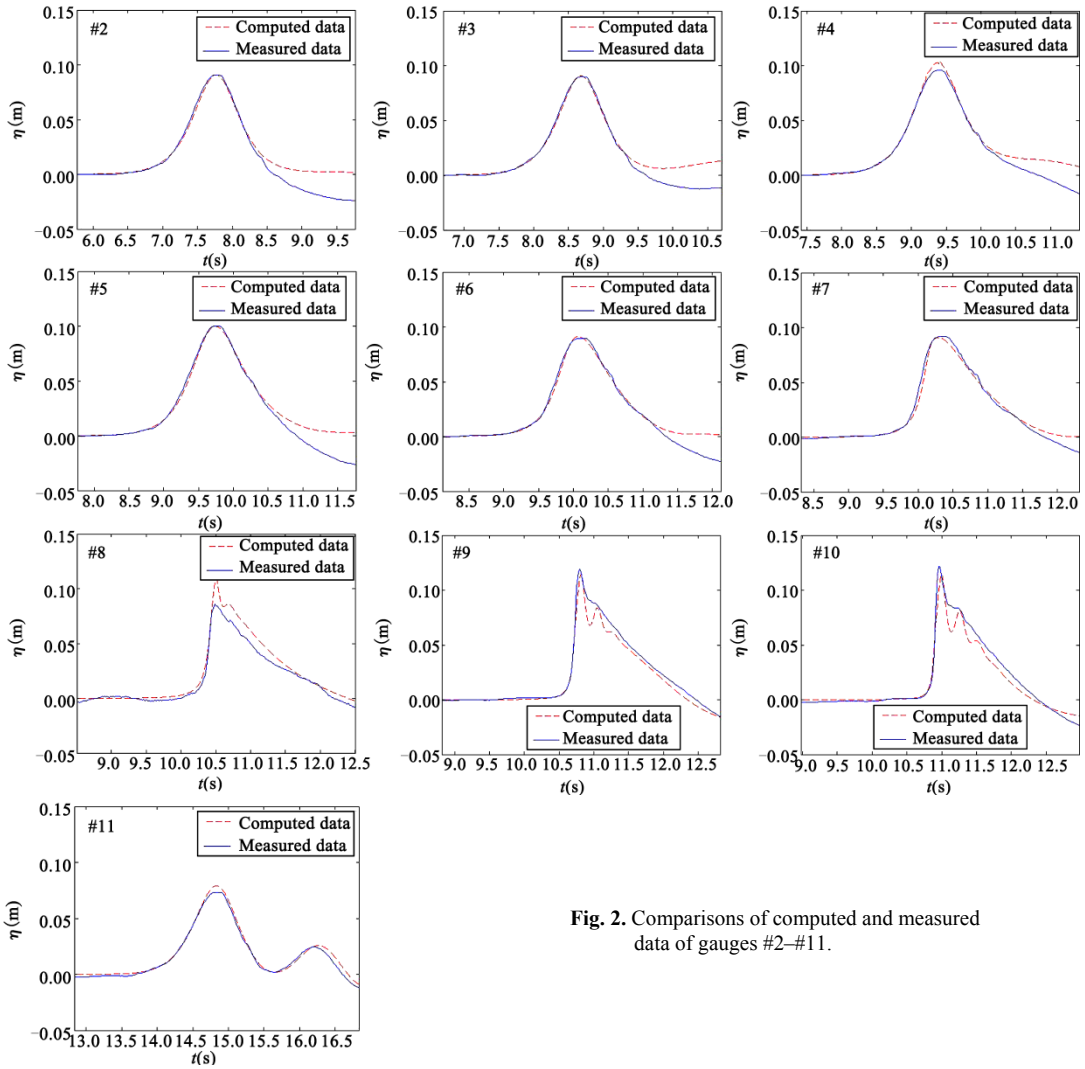

Fig. 2. Comparisons of computed and measured data of gauges #2–#11.

Solitary wave propagation through submerged breakwater can basically be divided into three parts: (1) Initial run-up motion (gauges #4, #5 and #6). In the solitary wave generation process, a series of dispersive waves followed solitary wave are formed inevitably (Wang *et al*., 2011). So the trailing of

the measured wave surface at gauges #2–#6 in Fig. 2 can be seen clearly. The trailing of computed data is not consistent with measured data. (2) Wave propagates through submerged breakwater. In this process, breaking happens at gauge #8. Because of the limitation of eddy viscosity to simulate wave breaking, the wave surface at breaking point cannot be simulated exactly. But the breaking point can be simulated accurately. (3) Wave reforms after solitary wave passing over the submerged breakwater. The computed data and the measured data at gauge #11 match very well. Fig. 2 shows that the model can simulate solitary wave run-up, overtopping, and reformation of wave behind the submerged breakwater. For the wave breaking, the model can simulate the location of surf zone accurately. It also can simulate wave reformation. It shows that the model can be applied to simulate solitary wave propagating through submerged breakwater.

In order to study the water particle velocity distribution, water depth was divided into five layers with six layer interfaces to simulate velocity at each layer interface by the model, and the simulated results and the solitary wave theoretical results were compared.

With the water depth d=40 cm, wave height H=10 cm as an example to verify the solitary wave velocity, the simulated results and theoretical results are shown in Figs. 3 and 4. The results show that the water particle of solitary wave only moves to wave propagation direction but never backward. Before the wave crest coming, water particle far from the wave crest (x=10h) has not yet moved, almost in stationary state. With the arrival of wave crest, water particle moves upward and forward (u, w are positive). When the wave crest passes, the horizontal velocity and the displacement of water particle reach the maximum value and the vertical velocity is 0. After the wave crest passing over, water particle begins to move downward (w is negative). The horizontal velocity gradually slows down and finally returns to the original water depth position. And the water particle has a net forward displacement in horizontal direction. In the whole process, the vertical velocity at bottom (z=0) is always 0. The closer the water particle to the surface, the bigger the movement amplitudes of the horizontal and vertical directions. The horizontal velocity and vertical velocity reach the maximum in the surface. Figs. 3 and 4 show that the simulated value and theoretical value of water particle velocity are very close. The model can be applied to simulate the water particle velocity.

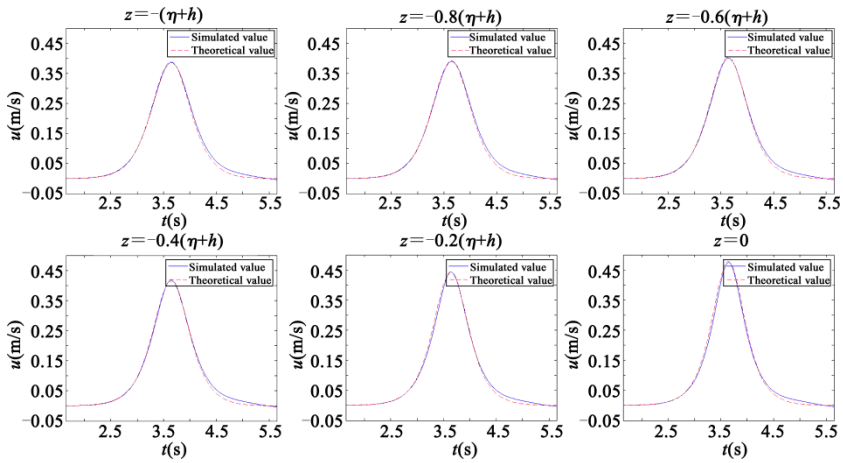

Fig. 3. Horizontal velocity comparisons of simulated results with theoretical results.

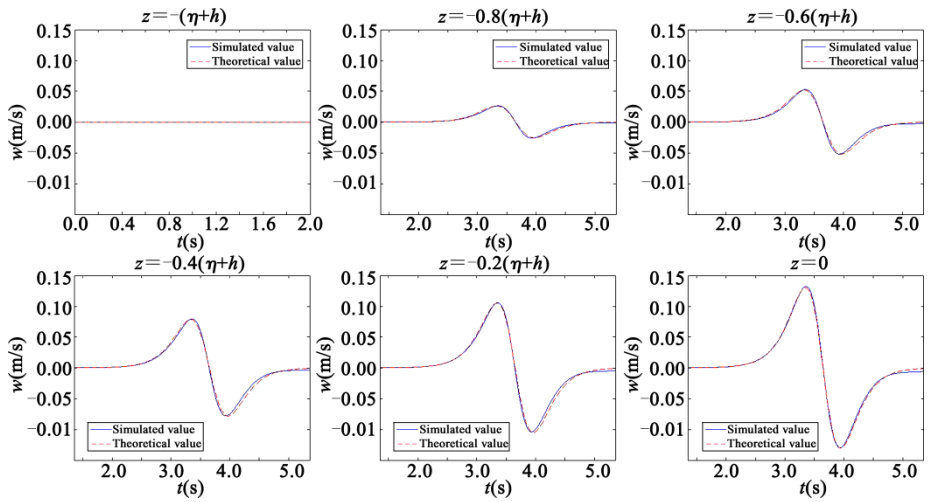

Fig. 4. Vertical velocity comparisons of the simulated results with theoretical results.

4. Analysis of Propagation Characteristics

4.1 Analysis of Wave Surface and Wave Spectra

As the solitary wave propagates from deep water to the submerged breakwater, the wave field is transformed due to the effects of shoaling, refraction, and reflection. The analysis of wave surface elevation changes cannot make understood of the propagation characteristics of solitary waves, so the wavelet amplitude spectra are given below.

The computed surface elevations and corresponding wavelet amplitude spectra are plotted in Fig. 5. In front of the submerged breakwater, there are three wave gauges (#1, #2, and #3). From Fig. 5, we can see that the reflected wave is formed in front of the breakwater, and the corresponding wavelet amplitude spectrum is stratified obviously being seen from the figures. The wavelet amplitude spectrum of gauge #1 shows several layers clearly, which is because the reflected wave propagates longer distance to gauge #1 and the reflected wave and incident wave are separated. Gauges #4, #5 and #6 show the run-up processes. In the process, solitary wave followed by a trough connecting it with the dispersive wave pattern is formed. The corresponding wavelet amplitude spectrum stratifies more and more obviously. The stratification at gauge #6 is the most obvious. Gauges #7, #8, #9 and #10 are wave gauges on the top of the breakwater. The figures show that solitary wave breaks at those gauges. Before breaking, the corresponding wavelet amplitude spectra become more and more concentrated. When the solitary wave breaks, enormous energy is released. Behind the breakwater (gauge #11), solitary wave followed by a series of dispersive waves are formed and the corresponding wavelet amplitude spectrum stratifies obviously and high-frequency wave appears.

Compared wave surface elevations from gauge #1 to gauge #11, we can obtain that solitary wave followed by a series of dispersive waves appears after it passes over the submerged breakwater, the corresponding wavelet amplitude spectra tend to rotate clockwise, and the reason is that the frequencies of solitary wave and dispersive wave are different. Therefore, the effect of the submerged

breakwater on solitary wave performs not only on wave surface, but also on spectra change.

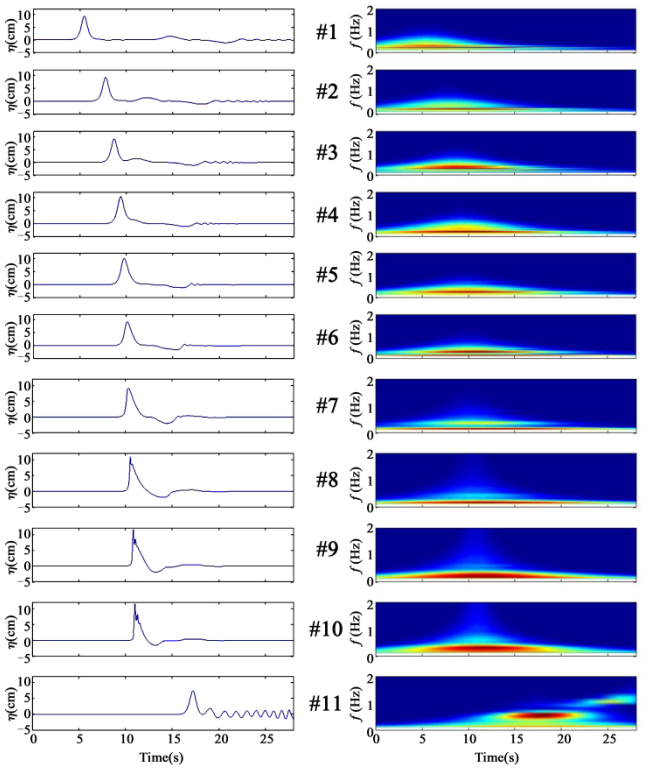

Fig. 5. computed surface elevations and corresponding wavelet amplitude spectra at gauges #1–#11.

The measured surface elevations and corresponding wavelet amplitude spectra are plotted in Fig. 6. In the solitary wave generation process, a series of dispersive waves followed solitary waves are formed inevitably. Comparing gauges #1, #2 and #3 of Fig. 5 with those of Fig. 6, and by analyzing the computed data and measured data comprehensively, we can see that a series of dispersive waves followed solitary waves in gauges #1, #2 and #3 of Fig. 6 are composed with the reflected wave and dispersive wave produced in the process of wave generation. The wave surface elevation and frequency of the measured solitary wave are consistent with the computed data except for the trailing wave. The surface elevation and frequency of computed data and measured data of gauges #4–#11 are very similar except for the component of dispersive wave.

4.2 Analysis of Velocity at Every Level

Based on the velocity analysis of gauges #1, #2 and #3, we can see that the surface velocity of water particles is larger than the bottom velocity in front of the submerged breakwater obviously. The maximum horizontal velocity at z=0 is 0.47 m/s; the maximum horizontal velocity at z= –(η+h) is 0.38 m/s; and the water particle vertical velocity at z= –(η+h) is 0. Solitary wave is a kind of progressive wave. Water particle only moves to wave propagation direction never backward. However, because of the reflection of submerged breakwater, there is a small velocity in the vertical direction besides

horizontal velocity (*u, w* sometimes are negative). The vertical velocity is almost 0 when the horizontal velocity is the maximum.

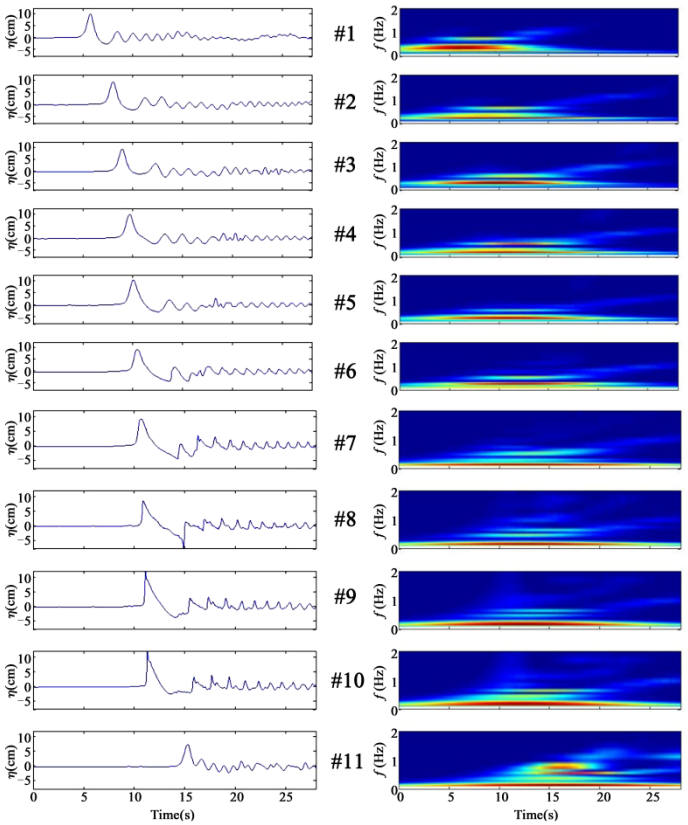

Fig. 6. Measured surface elevations and corresponding wavelet amplitude spectra at gauges #1–#11.

During solitary wave run-up, the time when the horizontal velocity of gauge #5 achieves the maximum at $z= -(\eta+h)$, $-0.8(\eta+h)$, $-0.6(\eta+h)$, $-0.4(\eta+h)$, $-0.2(\eta+h)$, 0 is 9.342, 9.35, 9.356, 9.36, 9.404, and 9.404 s, respectively. The surface elevation achieves the maximum at 9.414 s. In the process of run-up, the bottom layer horizontal velocity firstly achieves the maximum, and then the surface layer horizontal velocity, and finally, the surface elevation reaches the highest point. The maximum horizontal velocity at $z = 0$ is 0.52 m/s; the maximum horizontal velocity at $z= -(\eta+h)$ is 0.45 m/s; the bottom and surface horizontal velocities are different. There is a small velocity in the vertical direction at bottom level $z=-(\eta+h)$ because the bathymetry changes.

When the solitary wave propagates on the breakwater (gauges #6, #7, #8, #9 and #10), the velocity of surface layer first achieves the maximum. The time when the horizontal velocity of gauge #7 achieves the maximum at $z= -(\eta+h)$, $-0.8(\eta+h)$, $-0.6(\eta+h)$, $-0.4(\eta+h)$, $-0.2(\eta+h)$, 0 is 10.296, 10.294, 10.292, 10.268, 10.216, and 10.2 s, respectively. The horizontal velocity becomes larger than before and each layer interface has little difference. The vertical velocity at the bottom level $z= -(\eta+h)$ is 0. The horizontal velocity (1.46 m/s) and vertical velocity (0.55 m/s) achieve the maximum at gauge

#10 when the solitary wave is breaking.

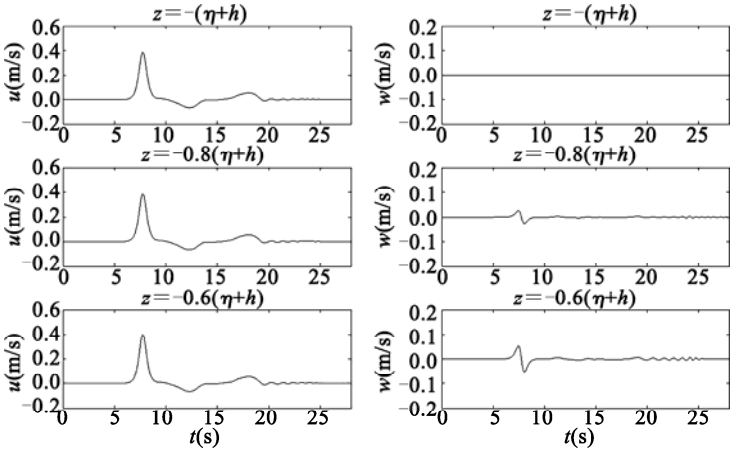

Fig. 7. Water particles horizontal velocity (left panel) and vertical velocity (right panel) at layer interfaces at gauge #2.

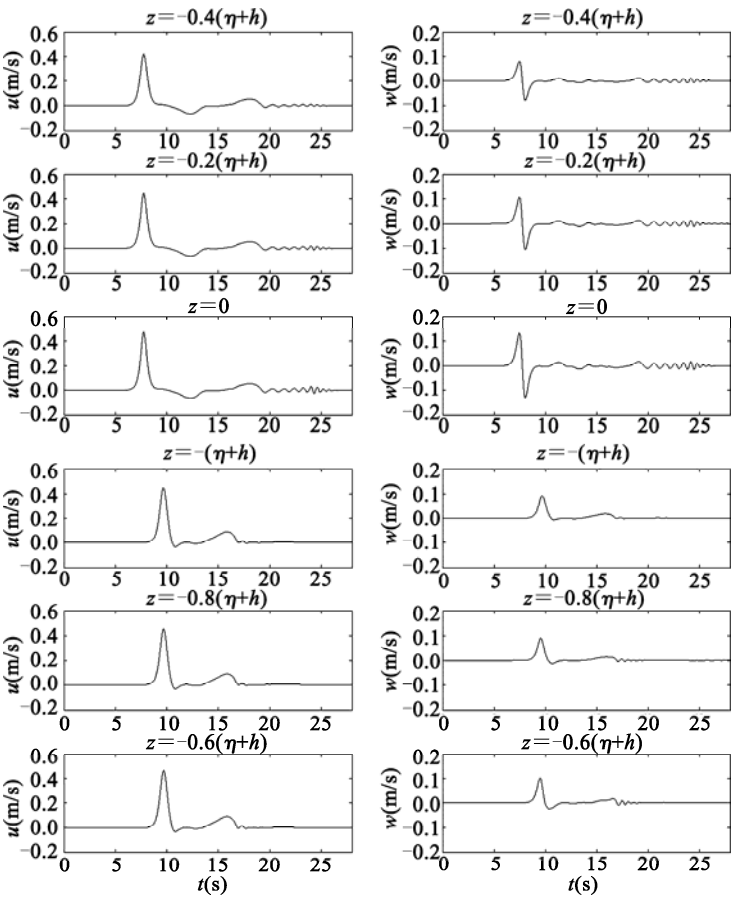

Fig. 8. Water particles horizontal velocity (left panel) and vertical velocity (right panel) at layer interfaces at gauge #5 (to be continued).

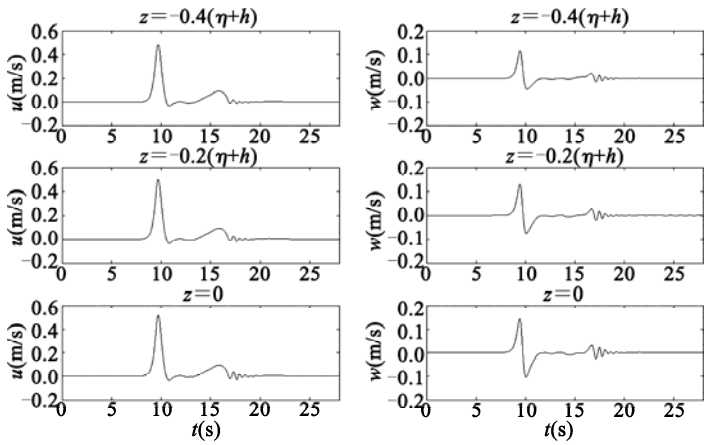

Fig. 8(continued). Water particles horizontal velocity (left panel) and vertical velocity (right panel) at layer interfaces at gauge #5.

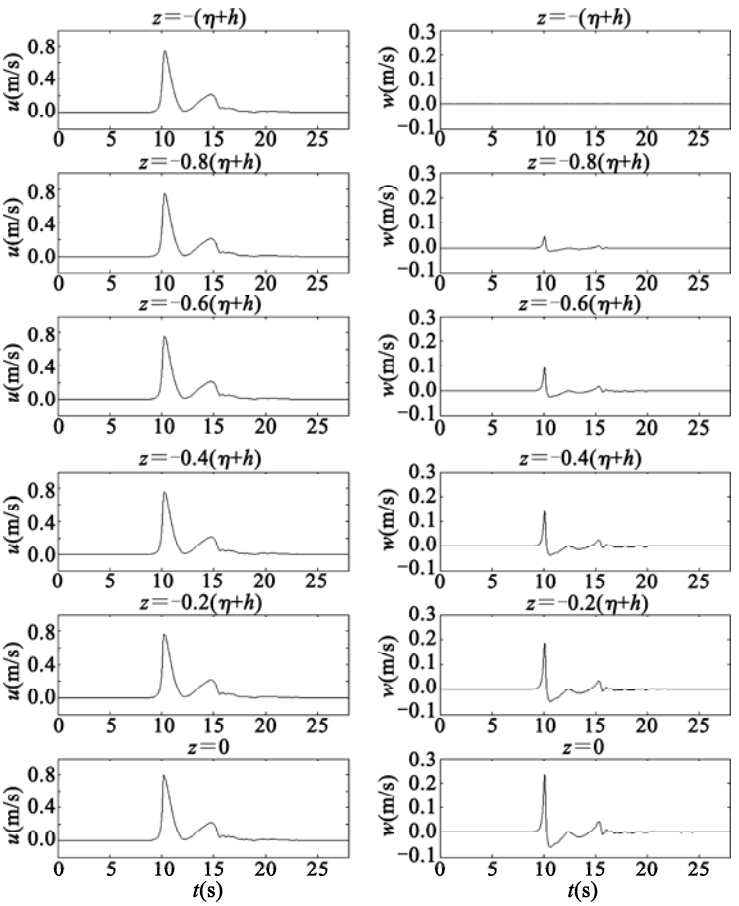

Fig. 9. water particles horizontal velocity (left panel) and vertical velocity (right panel) at layer interfaces at gauge #7.

Water particle velocity at each layer interface decreases obviously after passing through the

submerged breakwater. The surface layer velocity of water particle achieves the maximum firstly. Horizontal velocities at layer interfaces are close. The horizontal velocities at $z= -(\eta+h)$, $-0.8(\eta+h)$, $-0.6(\eta+h)$, $-0.4(\eta+h)$, $-0.2(\eta+h)$, and 0 are 0.318, 0.32, 0.33, 0.34, 0.36, and 0.39 m/s, respectively. The vertical velocity at $z= -(\eta+h)$ is 0.

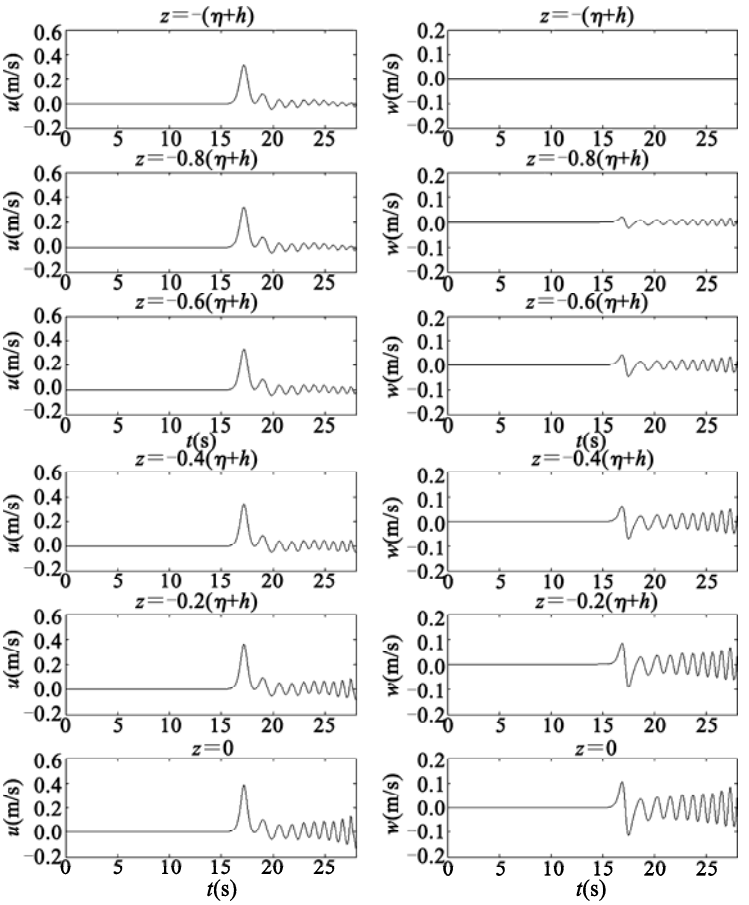

Fig. 10. Water particles horizontal velocity (left panel) and vertical velocity (right panel) at layer interfaces at gauge #11.

5. Conclusions

(1) The Boussinesq equation model can simulate the solitary wave run-up, overtopping and reformation of wave behind the submerged breakwater and also can simulate the water particle velocity. The model can be applied to simulate the solitary wave propagating through a submerged breakwater.

(2) We compare the simulated data with measured data and analyze surface elevations using wavelet transform method. Because different wave frequencies stratify in the wavelet amplitude spectra, we can divide the wave reflection in front of breakwater easily through layers in the wavelet amplitude spectra. Comparing wave surface elevations from gauge #1 to gauge #11, we can obtain the

solitary waves followed by a series of dispersive waves after they pass over the submerged breakwater. And the corresponding wavelet amplitude spectra tend to rotate clockwise.

(3) Horizontal velocity and vertical velocity at each layer interface in the process of solitary propagation through the submerged breakwater are analyzed. In front of the dike, the surface velocity is obviously larger than the bottom velocity in front of the submerged breakwater. The vertical velocity is small, and the vertical velocity at the bottom level is 0. During the run-up process, there is a small velocity in the vertical direction at the bottom level because the bathymetry changes. The bottom horizontal velocity firstly achieves the maximum, and then the surface layer horizontal velocity, and finally, the surface elevation reaches the highest point. When the solitary wave propagates on the breakwater, the surface layer velocity first achieves the maximum, and the horizontal velocity becomes larger than before and velocities at each layer interfaces have little difference. The water particle velocity at the layer interface decreases obviously after the solitary waves pass through the submerged breakwater. The surface layer velocity achieves the maximum firstly. The horizontal velocity of every level is close because of the turbulence caused by wave breaking.

References

Chen, Q., Kirby, J. T. and Dalrymple, R, A., 2000. Boussinesq modeling of wave transformation, breaking, and runup, I: 2D, *J. Waterw. Port Coast. Ocean Eng.*, ASCE, **126**(1): 48–56.

Dong, G. H., Wang, G., Ma, X. Z. and Ma, Y. C., 2010. Harbor resonance induced by subaerial landslide-generated impact waves, *Ocean Eng*., **37**(10): 927–934.

Grilli, S. T., Subramanya, R., Svendse, I. A. and Veeramony, J., 1994. Shoaling of solitary waves on plane beaches, *J. Waterw*. *Port Coast*. *Ocean Eng*., ASCE, **120**(6): 609–628.

Hara, M., Yasuda, T. and Sakakibara, Y., 1992. Characteristics of a solitary wave breaking caused by a submerged obstacle*, Proc. 23rd Int. Conf. Coast. Eng.* (*ICCE*), Venice, Italy.

Hsiao, S.-C. and Lin, T.-C., 2010. Tsunami-like solitary waves impinging and overtopping an impermeable seawall: Experiment and RANS modeling, *Coast. Eng*., **57**(1): 1–18.

Kennedy, A. B., Chen, Q. and Kirby, J. T., 2000. Boussinesq modeling of wave transformation, breaking, and runup, I: 1D, *J. Waterw. Port Coast. Ocean Eng.*, ASCE, **126**(1): 39–47.

Kim, N. H. and Ko, H. S., 2008. Numerical simulation on solitary wave propagation and run-up by SPH method, *KSCE J. Civil Eng.*, **4**, 221–226.

Li, Y. and Raichlen, F., 2001. Solitary wave run-up on plane slopes, *J. Waterw*. *Port Coast*. *Ocean Eng*., ASCE, **127**(1): 33–44.

Li, Y. and Raichlen, F., 2002. Non-breaking and breaking solitary wave run-up, *J. Fluid Mech.*, **456**, 295–318.

Massel, S. R., 2001. Wavelet analysis for processing of ocean surface wave records, *Ocean Eng*., **28**(8): 957–987.

Nwogu, O., 1993. Alternative form of Boussinesq equations for nearshore wave propagation, *J. Waterw*. *Port Coast*. *Ocean Eng*., ASCE, **119**(6): 618–638.

Panizzo, A., Bellotti, G. and De Girolamo, P., 2002. Application of wavelet transform analysis to landslide generated waves, *Coast. Eng.*, **44**(4): 321–338.

Penchev, V. and Shukrieva, S., 2007. Numerical simulation of waves in harbor areas – Example applications for Bulgarian Black Sea Coast, *Proc*. *4th Int. Conf.* "*Port Development and Coastal Environment*", Varna.

Synolakis, C. E., 1987. The run-up of solitary waves, *J. Fluid Mech.*, **185**, 523–545.

Wang, J., Wang, D. T., Zuo, Q. H. *et al.*, 2011. Study on characteristic of solitary wave simulation in library, *Proc .6th Int. Conf. on Asian and Pacific* (*APAC2011*), Hong Kong, China, 1738–1746.

Zelt, J. A., 1991. The run-up of non-breaking and breaking solitary waves, *Coast. Eng*., **15**(3): 205–246.